

Supporting Information

Superior Supercapacitive Performance of Grass-like CuO Thin Films Deposited by Liquid Phase Deposition

Shreelekha N. Khatavkar and Shrikrishna D. Sartale*

Thin Films and Nanomaterials Laboratory,
Department of Physics, SavitribaiPhule Pune University,
Pune - 411007, India.

*Corresponding author's email: sdsartale@physics.unipune.ac.in

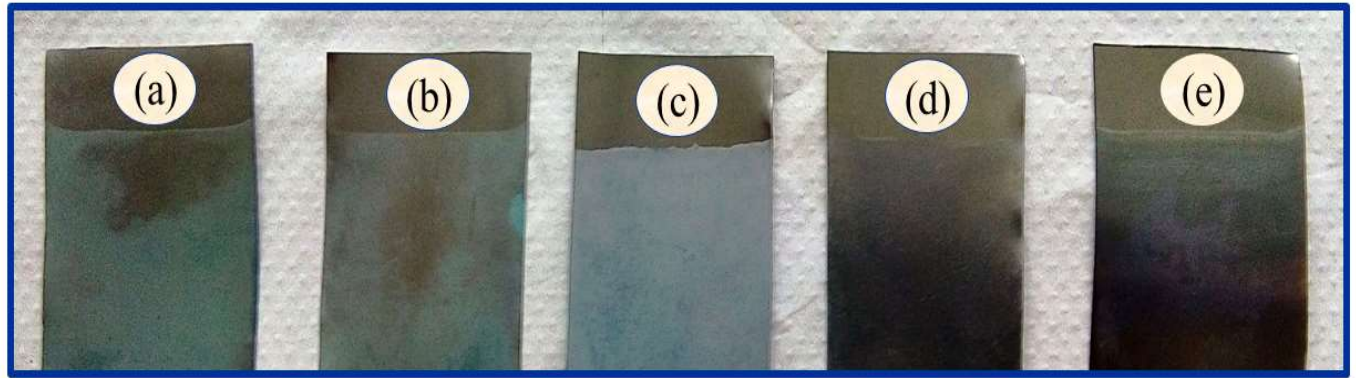


Figure S1. Photo of as-deposited films on flat SS with varying boric acid (H_3BO_3) concentrations: (a) 0.05, (b) 0.1, (c) 0.5, (d) 1 and (e) 1.5 M.

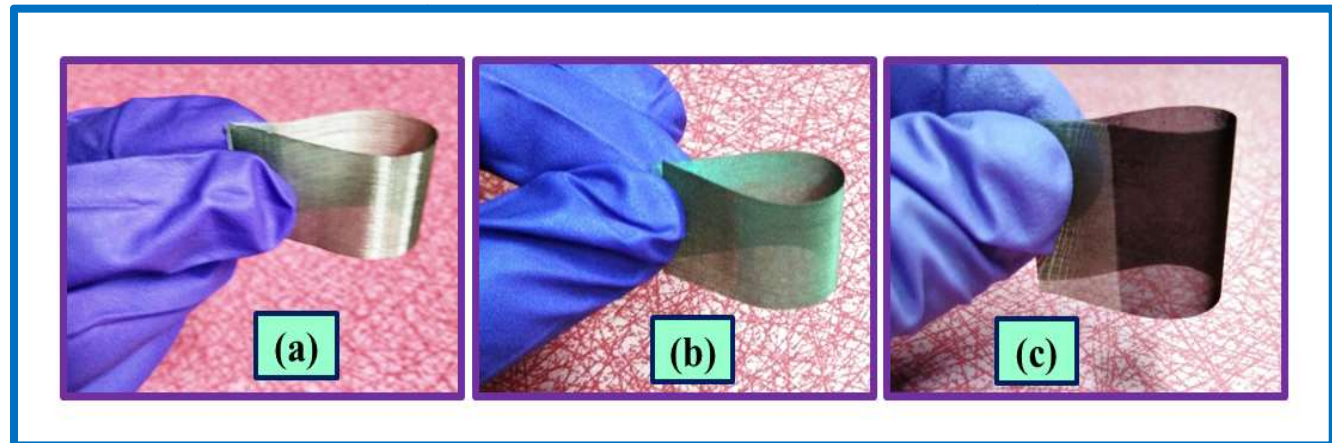


Figure S2. Photos of light weight and flexible SS mesh, (a) before deposition, (b) after deposition and (c) same film annealed at 300 °C, for 1 h.

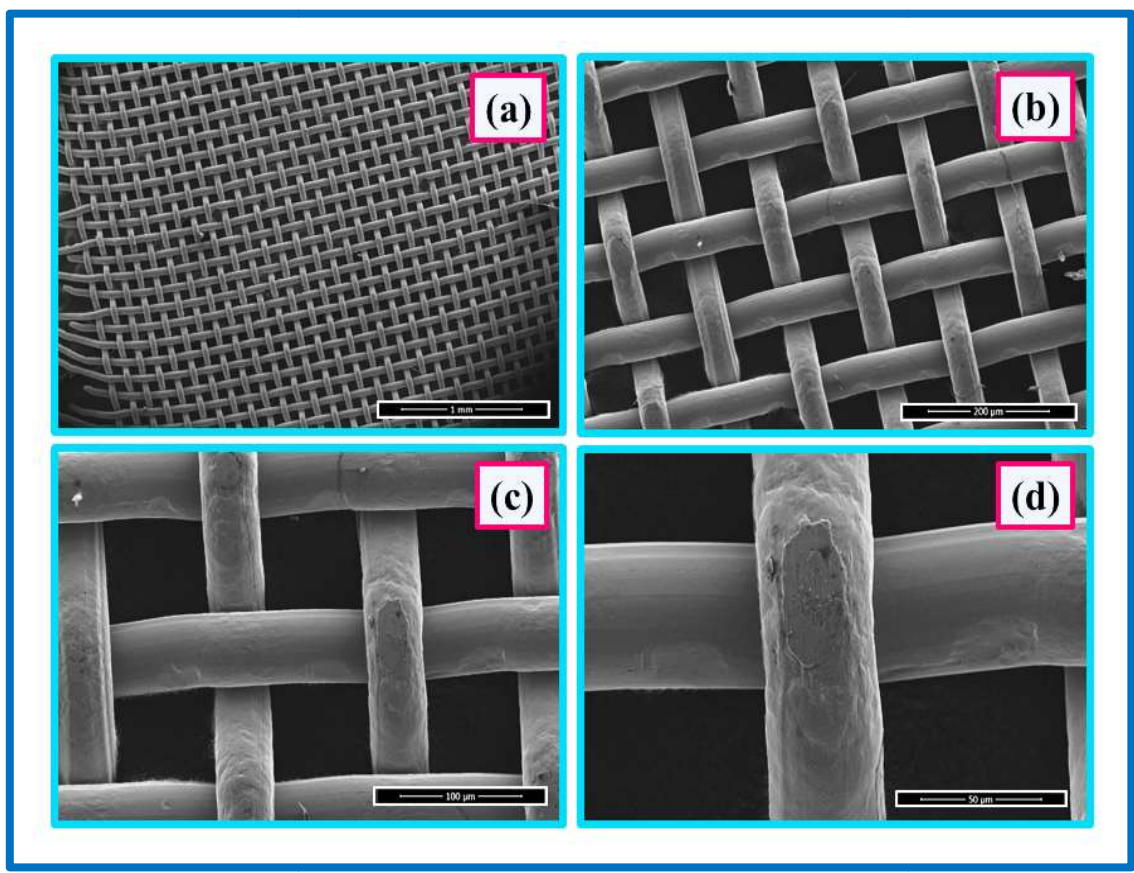


Figure S3. FE-SEM images of the bare SS mesh at four different magnifications.

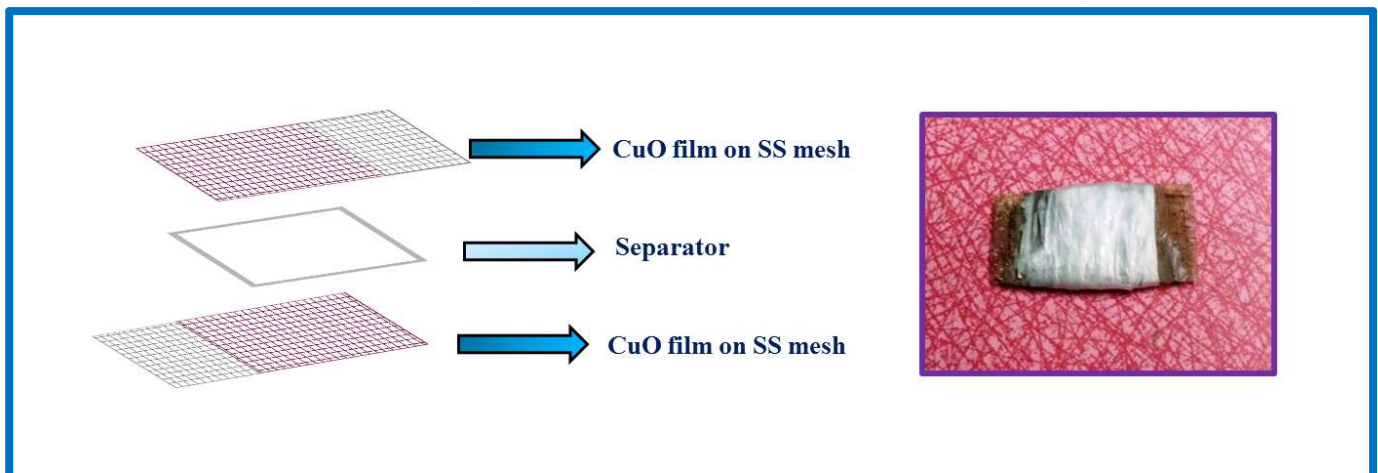


Figure S4. Schematic and actual photo of the fabricated CuO symmetric device.

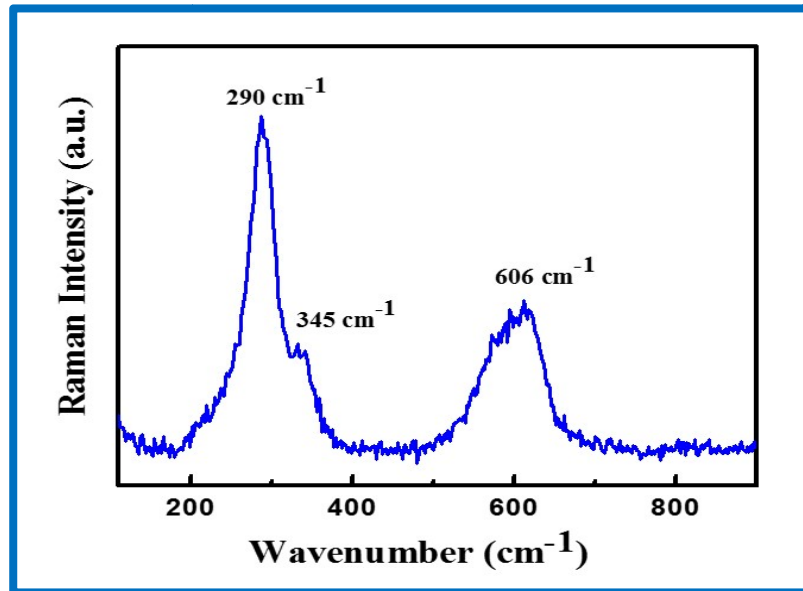


Figure S5. Raman spectrum of film annealed at 300 °C CuO on SS mesh. All the raman peaks are assigned to CuO phase.

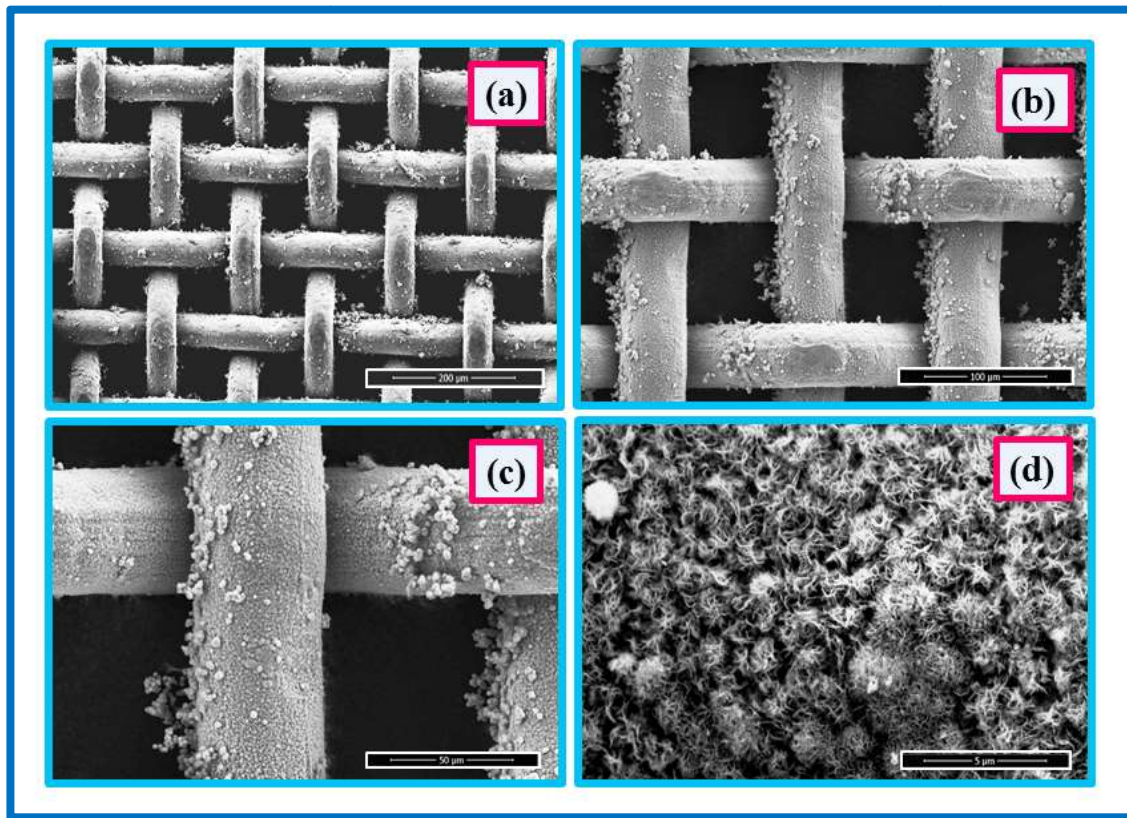


Figure S6. FE-SEM images of the CuO on SS mesh at four different magnifications.

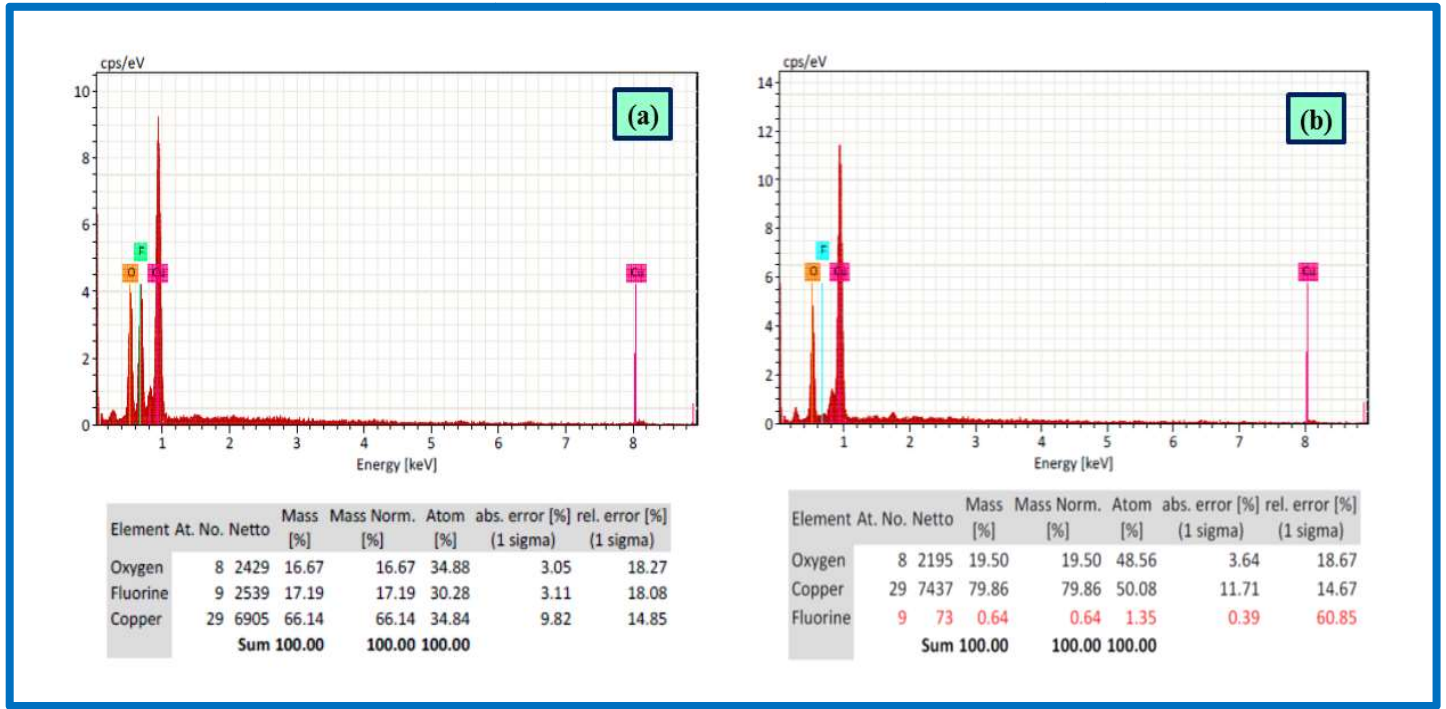


Figure S7. Energy dispersive spectroscopy (EDS) of a) as-deposited and b) annealed at 300 °C film.

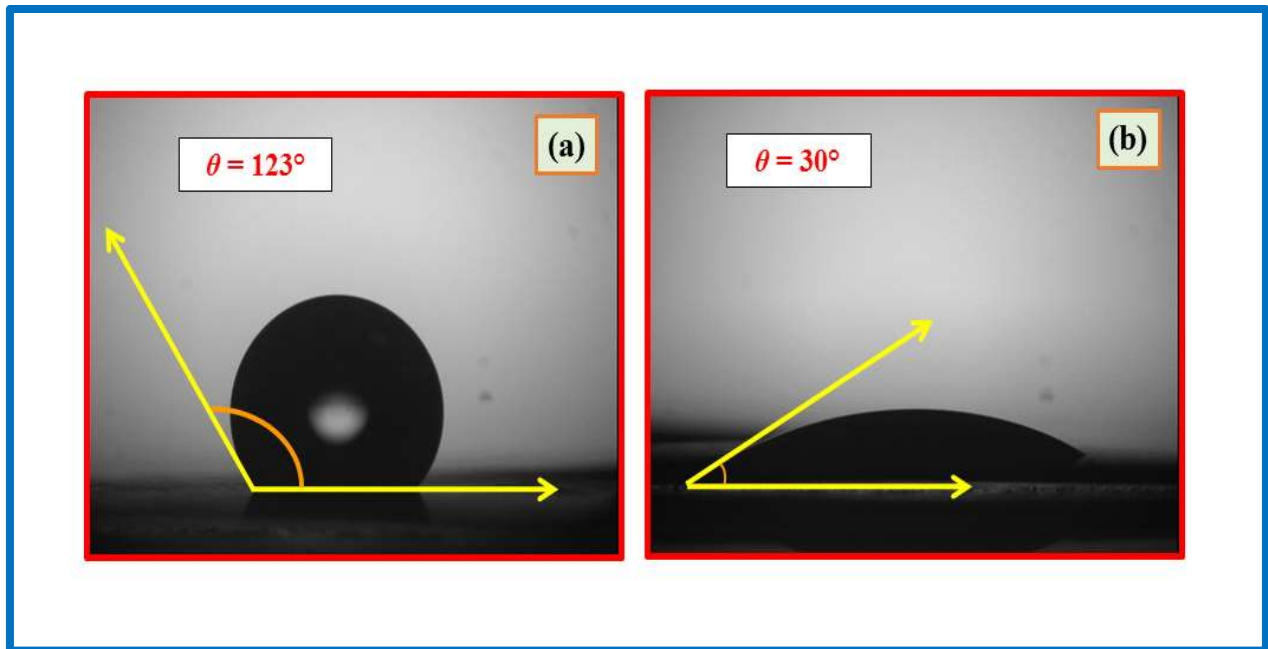


Figure S8. Water contact angle measurement of the a) as-deposited and b) annealed at 300°C film on flat SS.

➤ **Estimation of specific capacitance from CV curves:**

From CV curves, specific capacitance (C_s) associated with the CuO electrode was calculated using the following relation

$$C_s = \int I dV / (V \times v \times m) \dots \dots (S1)$$

where,

C_s : specific capacitance ($F g^{-1}$),

I : response current (mA),

V : potential window (V),

v : voltage scan rate ($mV s^{-1}$),

m : mass of the active electrode material dipped in the electrolyte (g).

➤ **Estimation of specific capacitance from charge-discharge curves:**

The specific capacitance, C_s of CuO electrode was calculated from the charge-discharge curves by the relation

$$C_s = (I \times t_d) / (V \times m) \dots \dots (S2)$$

$$SE = 0.5 (C_s \times V^2) \dots \dots (S3)$$

$$SP = SE / t_d \dots \dots (S4)$$

where,

C_s : specific capacitance ($F g^{-1}$),

I : current (mA),

V : potential window (V),

t_d : discharging time (s),

m : mass of the active material dipped in the electrolyte (g),

SE : specific energy ($Wh kg^{-1}$),

SP : specific power ($kW kg^{-1}$),

➤ **Estimation of specific capacitance from EIS:**

The specific capacitance, C_s of CuO electrode was calculated from the EIS using the relations

$$C(\omega) = C'(\omega) + C''(\omega) \dots\dots (S5)$$

$$C' = -Z'' / (\omega |Z|^2 \times m) \dots\dots (S6)$$

$$C'' = Z' / (\omega |Z|^2 \times m) \dots\dots (S7)$$

where,

$C(\omega)$: total capacitance ($F g^{-1}$),

C' : real capacitance component ($F g^{-1}$),

C'' : imaginary capacitance component ($F g^{-1}$),

$Z(\omega)'$: real impedance component (Ω),

$Z(\omega)''$: imaginary impedance component (Ω),

$|Z|$: modulus of $Z = [(Z')^2 + (Z'')^2]^{1/2}$, (Ω)

ω : angular frequency($2\pi f$), (Hz)

f : frequency (Hz),

m : mass of the active material dipped in the electrolyte (g).

➤ **Estimation of Electrochemical active specific surface area from EIS:**

The electrochemical active specific surface area of CuO electrode was calculated from the EIS using the relations

$$S_E = C_{dm} / C_d \dots\dots (S8)$$

$$C_{dm} = 1 / (2\pi m f Z_{Img}) \dots\dots (S9)$$

where,

S_E : electrochemical active specific surface area ($m^2 g^{-1}$),

C_{dm} : specific capacitance of the electrochemical double layer obtained from impedance spectroscopy at low frequency ($F g^{-1}$),

C_d : capacitance of the electrochemical double layer with a constant value of $20 \mu F cm^{-2}$,

m : mass of the active material dipped in the electrolyte (g),

f : frequency in the low frequency range (0.01 Hz),

Z_{Img} : imaginary part of the impedance (Ω).

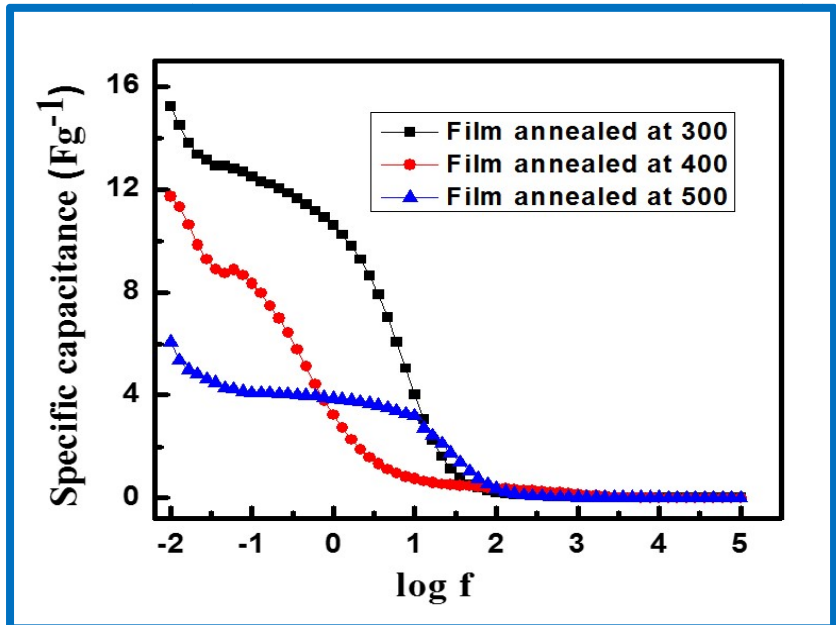


Figure S10. Specific capacitance against $\log f$ of the annealed films (CuO on flat SS) at 300, 400 and 500 °C.

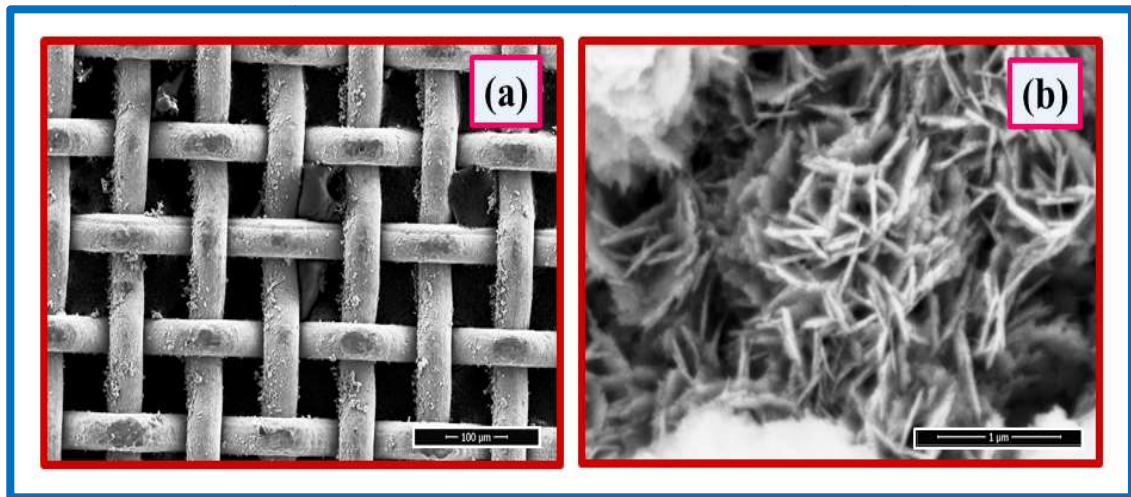


Figure S11. FE-SEM of the CuO on SS mesh electrode after 1000 cycles of cyclic voltammetry with two different magnifications.

Table: Supercapacitive performance of the CuO thin film electrode based on charge-discharge studies.

| Sr. No. | Synthesis method | Substrate | Morphology | Electrolyte | Current density | Maximum Specific capacitance (F g^{-1}) | Reference |
|---------|--|-------------|--|-------------------------------------|-------------------------|--|--------------|
| 1 | LPD | SS | CuO Bunch of grass | 6 M KOH | 2 mA cm ⁻² | 22 | Present work |
| 2 | Liquid solid reaction | Copper foil | CuO microflowers | 6 M KOH | 5 mA cm ⁻² | 30 | 1 |
| 3 | LPD | Mesh SS | CuO - nanograss | 6 M KOH | 2 mA cm ⁻² | 59 | Present work |
| 4 | Potentio-dynamic deposition | SS | CuO cauliflower | 1 M Na ₂ SO ₄ | 2 mA cm ⁻² | 162 | 2 |
| 5 | Anodization | Copper foam | CuO nanosheets | 6 M KOH | 0.4 mA mg ⁻¹ | 212 | 3 |
| 6 | Reactive sputtering | SS | Compact Cu ₂ O | 6 M KOH | 1.5 Ag ⁻¹ | 220 | 4 |
| 7 | Reactive sputtering | SS | Granular porous CuO | 6 M KOH | 1.5 Ag ⁻¹ | 260 | 4 |
| 8 | Liquid-solid reaction | Copper foil | Lotus like CuO | 5 M NaOH | 2 mA cm ⁻² | 278 | 5 |
| 9 | Chemical bathe deposition (CBD) | SS | CuO Nanobud clusters | 1 M Na ₂ SO ₄ | 0.5 mA cm ⁻² | 391 | 6 |
| 10 | CBD | SS | CuO Micro-woolen | 1 M Na ₂ SO ₄ | 0.5 mA cm ⁻² | 340 | 7 |
| 11 | CBD | SS | CuO/(OH) ₂ nanobuds | 1 M KOH | 1 mA cm ⁻² | 340 | 8 |
| 12 | CBD | SS | CuO Micro-woolen | 1 M Na ₂ SO ₄ | 1 mA cm ⁻² | 400 | 9 |
| 13 | Surfactant mediated CBD | SS | CuO- flower like | 1 M Na ₂ SO ₄ | 0.5 mA cm ⁻² | 413 | 10 |
| 14 | Successive ionic layer adsorption and reaction (SILAR) | SS | NanoFlowers-like CuO/Cu(OH) ₂ | 2 M KOH | 1 mA cm ⁻² | 457 | 11 |
| 15 | Template free growth method | Nickel foam | CuO-nanosheet arrays | 6 M KOH | 5 mA cm ⁻² | 569 | 12 |

| | | | | | | | |
|----|-------------------------|-------------|--|-------------------------------------|-------------------------|-----|----|
| 16 | Liquid-solid reaction | Copper foil | Nanowire-like Cu(OH) ₂ arrays | 6 M KOH | 2 mA cm ⁻² | 750 | 1 |
| 17 | RF magnetron sputtering | SS | Nanograins | Phosphate-buffered aqueous solution | 0.5 mA cm ⁻² | 908 | 13 |
| 18 | In situ anodization | Copper foam | Graphene like CuO nanofilms | 3 M KOH | 1 A g ⁻¹ | 919 | 14 |

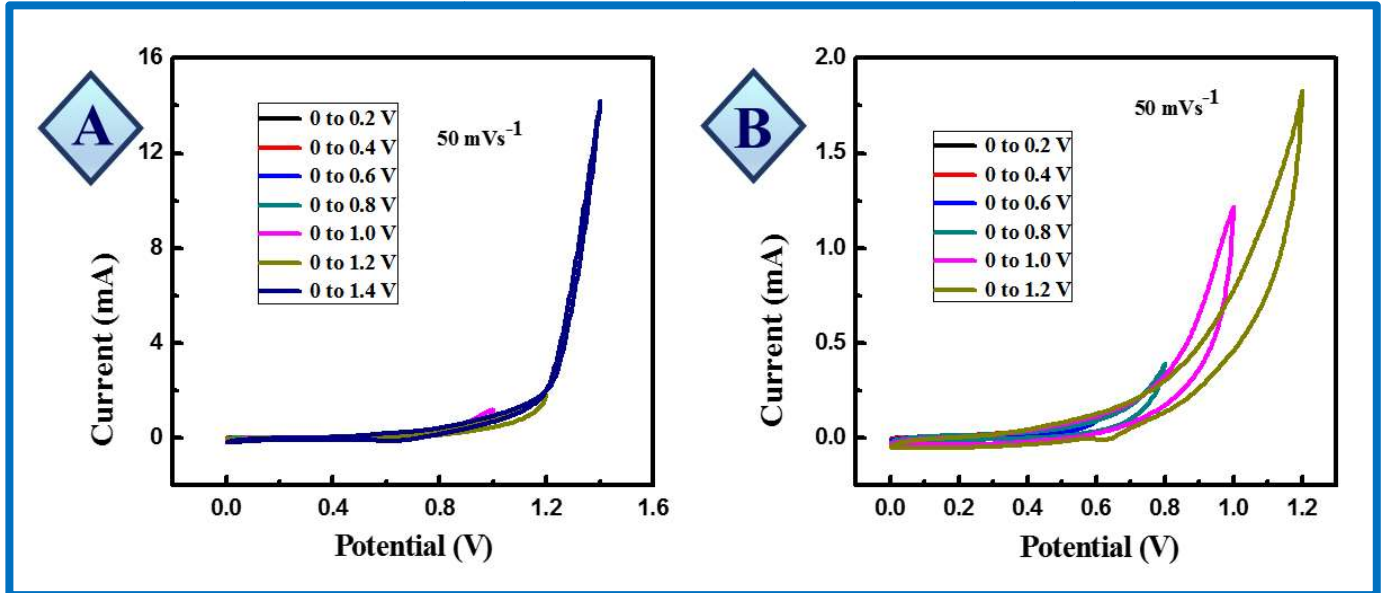


Figure S13. A) The CV of the CuO symmetric device at constant scan rate 50 mVs^{-1} in different potential ranges (0 to 0.2, 0.4, 0.6, 0.8, 1.0, 1.2 and 1.4 V) and B) Enlarged view of the CV (0 to 0.2, 0.4, 0.6, 0.8, 1.0 and 1.2 V).

S14: Table of comparison for CuO symmetric devices on two electrode system

| Sr. No. | Material and Method of preparation of symmetric device | Substrate | Gel Electrolyte/ Electrolyte | Scan rate / Current density | Maximum Specific capacitanc e (F g^{-1}) | Energy density and Power density | Cyclic stability (%) | Reference |
|------------|---|----------------|------------------------------------|---|--|---|----------------------------|-----------------|
| 1 | CuO CBD (Binder-free) | SS | CMC- Na_2SO_4 | 5 mV s^{-1} | ~ 9.5 | $\sim 35 \text{ Wh kg}^{-1}$ and $\sim 800 \text{ KWkg}^{-1}$ | 90 (1000 cycles) | 9 |
| 2 | CuO LPD (Binder-free) | Mesh SS | PVA-KOH | 5 mV s^{-1} | 22 | 0.6 Wh kg^{-1} and 1339 W kg^{-1} | 80 (1000 cycles) | Present work |
| 3 | CuO/RGO Hydrothermal (With Binder) | Nickel foam | 0.5M K_2SO_4 | 2 mV s^{-1} and 0.2 Ag^{-1} | 64 and 97 | 19 Wh kg^{-1} and 72 Wkg^{-1} . | - | 15 |

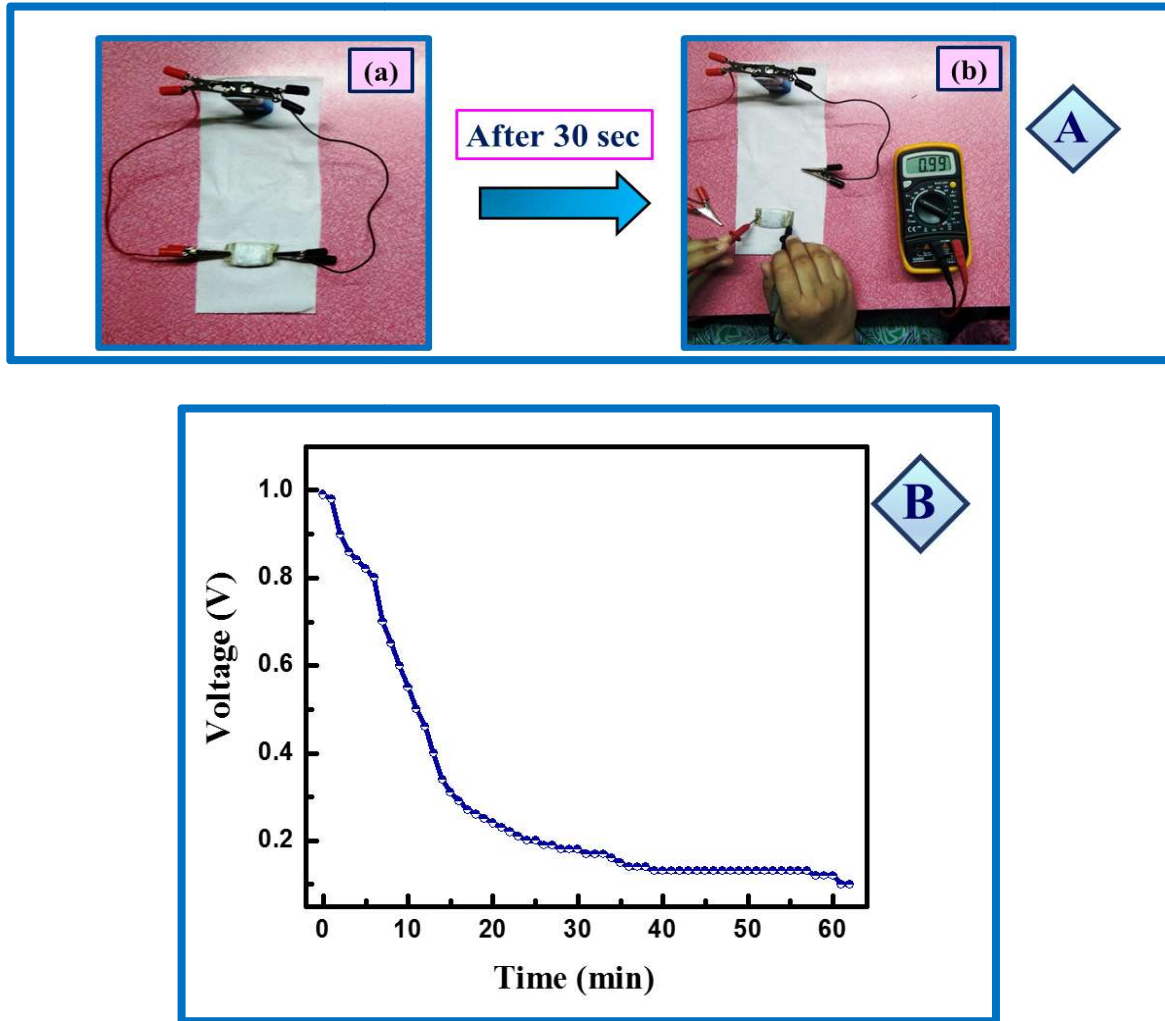


Figure S15. A) Demonstration of the fabricated symmetric device- (a) charging and (b) discharging of CuO symmetric device and B) Discharging voltage versus time for CuO symmetric device.

References

1. P. Xu, K. Ye, M. Du, J. Liu, K. Cheng, J. Yin, G. Wang and D. Cao, *RSC Adv*, 2015, **5**, 36656-36664.
2. D. P. Dubal, G. S. Gund, C. D. Lokhande and R. Holze, *Mater Res Bull*, 2013, **48**, 923-928.
3. Y. Li, S. Chang, X. Liu, J. Huang, J. Yin, G. Wang and D. Cao, *Electrochim Acta*, 2012, **85**, 393-398.
4. S. M. Pawar, J. Kim, A. I. Inamdar, H. Woo, Y. Jo, B. S. Pawar, S. Cho, H. Kim and H. Im, *Scientific reports*, 2016, **6**, 21310.
5. Y.-K. Hsu, Y.-C. Chen and Y.-G. Lin, *Journal of Electroanalytical Chemistry*, 2012, **673**, 43-47.
6. D. P. Dubal, G. S. Gund, R. Holze and C. D. Lokhande, *Journal of Electroanalytical Chemistry*, 2014, **712**, 40-46.
7. D. P. Dubal, G. S. Gund, R. Holze and C. D. Lokhande, *J Power Sources*, 2013, **242**, 687-698.
8. U. M. Patil, M. S. Nam, S. C. Lee, S. Liu, S. Kang, B. H. Park and S. C. Jun, *J Alloy Compd*, 2017, **701**, 1009-1018.
9. A. V. Shinde, N. R. Chodankar, V. C. Lokhande, A. C. Lokhande, T. Ji, J. H. Kim and C. D. Lokhande, *Rsc Adv*, 2016, **6**, 58839-58843.
10. D. P. Dubal, G. S. Gund, R. Holze, H. S. Jadhav, C. D. Lokhande and C. J. Park, *Dalton Transactions*, 2013, **42**, 6459-6467.
11. S. K. Shinde, D. P. Dubal, G. S. Ghodake, D. Y. Kim and V. J. Fulari, *Journal of Electroanalytical Chemistry*, 2014, **732**, 80-85.

12. G. Wang, J. Huang, S. Chen, Y. Gao and D. Cao, *J Power Sources*, 2011, **196**, 5756-5760.
13. B. Purusottam Reddy, K. Sivajee Ganesh and O. M. Hussain, *Applied Physics A*, 2016, **122**.
14. Y. Lu, X. Liu, K. Qiu, J. Cheng, W. Wang, H. Yan, C. Tang, J.-K. Kim and Y. Luo, *ACS Appl Mater Inter*, 2015, **7**, 9682-9690.
15. K. K. Purushothaman, B. Saravanakumar, I. M. Babu, B. Sethuraman and G. Muralidharan, *RSC Adv*, 2014, **4**, 23485.